ENAE743

Applied Nonlinear Control of Aerospace Systems

Final Project

Robust Control Of Bevel-Tipped Needle

ADITYA VARADARAJ

(UID: 117054859)

(SECTION: 0101)

M.Eng. Robotics (PMRO),

University of Maryland - College Park, College Park, MD - 20742, USA.

Date of Submission: 10th May, 2022

LIST OF FIGURES

CONTENTS

I. Introduction

In minimal invasive surgeries involving biopsy and brachytherapy procedures, needle is a commonly used tool employed for treatment. In such procedures, accuracy is a major requirement for the needle in reaching the target tissue region in spite of perturbations from neighboring tissues during needle maneuvering. In the current clinical scenarios, the target accuracy is limited by several factors mostly due to fatigue and human error. Also, during the needle insertion, physicians face several challenges such as the patient's movement, issue deformation, and dependence of human hand-eye coordination to insert the needle. Hence, accurate control is needed.

During insertion, due to the beveled tip, an asymmetric force is applied by the tissue on the needle, causing the needle tip to bend. Generally, during needle steering, base manipulation involves both spinning and insertion degrees of freedom. Thus, the spinning of the needle shaft alone controls the direction of the tip bending. Likewise, the insertion of the needle causes its tip to bend due to the tissue reaction force thereby following a curvilinear path. These bevel-tip needles generally have higher maneuverability compared to conventional rigid straight needles The merits of sliding mode based robust control strategies involve disturbance rejection, parameter uncertainty, and unmodeled dynamics, which are essential for addressing any practical applications.

Duty cycle spinning methods too have been used in the past [11]. Many papers have used Sliding-Mode control techniques to drive steerable needle [8] [9] [10].

The main paper whose results are reproduced in this project is [1].

Objectives of the paper [1]:

- To implement robust SMC that rejects disturbance
- Avoid Chattering using ISMC + STA and a Continuous Control

II. Methodology

A. Kinematic Model and State-Space Equation

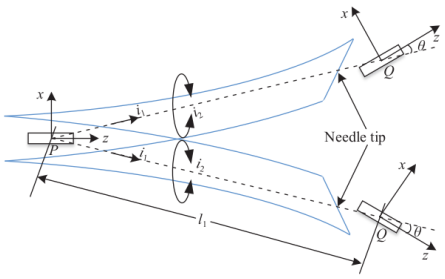

Fig. 1. Unicycle model of Steerable Needle [3] [1]

g_{PQ} is the homogeneous transformation matrix between points P and Q in Fig. 1. R_{PQ} and p_{PQ} are rotation matrix and translation vector respectively. The insertion velocity of needle i_1 and rotational (spinning) velocity of needle i_2 are the control inputs out of which i_1 is assumed to be constant ($i_1 = 1$) for the purpose of this paper.

i_1 causes the needle to move forward in z axis and curve itself about y axis at the same time. i_2 is responsible for keeping the needle movement along a straight path. $\dot{p_1}$ and $\dot{p_2}$ determine which components of the needle tip's velocity are affected by i_1 and i_2 and how. Curvature of needle is given by $k = \frac{\tan\theta}{l_1}$. For this paper [1], curvature is kept constant at $k = \frac{1}{56.7}\ cm^{-1}$.

$$
\begin{aligned}
g_{PQ} &= \begin{bmatrix} R_{PQ} & p_{PQ} \\ 0 & 1 \end{bmatrix} \in SE(3) \\
Velocity,\ v &= \dot{p_1} i_1 + \dot{p_2} i_2 \\
\dot{p_1} &= \begin{bmatrix} 0 & 0 & 1 & 0 & k & 0 \end{bmatrix}^T,\ \dot{p_2} = \begin{bmatrix} 0 & 0 & 0 & 0 & 0 & 1 \end{bmatrix}^T \\
v &= J\dot{q},\ q = \begin{bmatrix} x & y & z & \alpha & \beta & \gamma \end{bmatrix}^T
\end{aligned}
\tag{1}
$$

, where, $q = \begin{bmatrix} x & y & z & \alpha & \beta & \gamma \end{bmatrix}^T \in U \subset \Re^6$, α, β, γ are rotations about Z, Y and X axes respectively. $U = \{q \in \Re^6 \mid \beta \in \Re\ mod\ 2\pi,\ \alpha, \gamma \in \left(\frac{-\pi}{2}, \frac{\pi}{2}\right)\}$.

$$
\begin{aligned}
J &= \begin{bmatrix} R^T & 0_{3\times3} \\ 0_{3\times3} & J_{22} \end{bmatrix},\ J_{22} = \begin{bmatrix} -\sin\gamma\cos\alpha & \cos\gamma & 0 \\ \cos\gamma\cos\alpha & \sin\gamma & 0 \\ \sin\alpha & 0 & 1 \end{bmatrix} \\
\dot{q} &= J^{-1}\dot{p_1} i_1 + J^{-1}\dot{p_2} i_2 = \begin{bmatrix} \cos\alpha\sin\beta & 0 \\ -\sin\alpha & 0 \\ \cos\alpha\cos\beta & 0 \\ k\cos\gamma\sec\alpha & 0 \\ k\sin\gamma & 0 \\ -k\cos\gamma\tan\alpha & 1 \end{bmatrix} \begin{bmatrix} i_1 \\ i_2 \end{bmatrix}
\end{aligned}
\tag{2}
$$

The states x and z need not be controlled to stabilize needle in x-z plane. Moreover, the remaining states are not perturbed by specific coordinates (x, z). Thus, the state vector s is considered as given below with s_1 as the distance y from x-z plane, s_2 as the rotation (**yaw**) α about z-axis and s_3 as rotation (**roll / spinning**) γ about x-axis. Variable control input $i = i_2$.

$$
\begin{aligned}
s &= [s_1\ s_2\ s_3]^T = [y\ \alpha\ \gamma]^T \\
\dot{s_1} &= -\sin s_2 \\
\dot{s_2} &= k\cos s_3 \sec s_2 \\
\dot{s_3} &= -k\cos s_3 \tan s_2 + i \\
\Rightarrow\ \dot{s} &= f_0(s) + g_0(s) i \\
,\ where,\ f_0(s) &= \begin{bmatrix} -\sin s_2 \\ k\cos s_3 \sec s_2 \\ -k\cos s_3 \tan s_2 \end{bmatrix},\ g_0(s) = \begin{bmatrix} 0 \\ 0 \\ 1 \end{bmatrix}
\end{aligned}
\tag{3}
$$

As can be seen from the Fig. 2, the desired equilibrium point to restrict motion to x-z plane is $s = \begin{bmatrix} 0 & 0 & \frac{\pi}{2} \end{bmatrix}^T$.

Note: In the paper [1], the desired equilibrium is misprinted or wrongly written as $s = \begin{bmatrix} 0 & 0 & 0 \end{bmatrix}^T$. It should actually be $s = \begin{bmatrix} 0 & 0 & \frac{\pi}{2} \end{bmatrix}^T$.

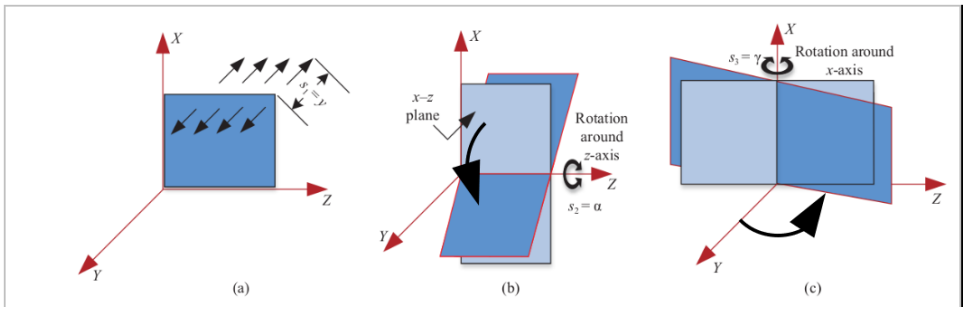

Fig. 2. States s_1, s_2 and s_3 [1]

B. Input-Output Feedback Linearization

Consider the output $\psi = h(s) = [1\ 0\ 0]s = s_1$.

$$\dot{s} = f_0(s) + g_0(s)i$$

$$, \ where, \ f_0(s) = \begin{bmatrix} -\sin s_2 \\ k \cos s_3 \sec s_2 \\ -k \cos s_3 \tan s_2 \end{bmatrix}, \ g_0(s) = \begin{bmatrix} 0 \\ 0 \\ 1 \end{bmatrix}$$

$$\psi = h(s) = [1\ 0\ 0]s = s_1$$

$$\dot{\psi} = \dot{s_1} = -\sin s_2$$

$$\ddot{\psi} = -\dot{s_2} \cos s_2 = -k \cos s_3$$

$$\frac{d\ddot{\psi}}{dt} = -k^2 \sin s_3 \cos s_3 \tan s_2 + k \sin s_3 i$$

$$\dot{\psi} = \frac{\delta h(s)}{\delta s}[f_0(s) + g_0(s)i] \tag{4}$$

$$\Rightarrow \ L_{f_0}h(s) = \frac{\delta h(s)}{\delta s} f_0(s) = \dot{\psi} = -\sin s_2$$

$$L_{g_0}h(s) = \frac{\delta h(s)}{\delta s} g_0(s) = 0$$

$$L_{f_0}^2 h(s) = \frac{\delta L_{f_0}h(s)}{\delta s} f_0(s) = \begin{bmatrix} 0 & -\cos s_2 & 0 \end{bmatrix} \begin{bmatrix} -\sin s_2 \\ k \cos s_3 \sec s_2 \\ -k \cos s_3 \tan s_2 \end{bmatrix} = -k \cos s_3$$

$$L_{g_0}L_{f_0}h(s) = \frac{\delta L_{f_0}h(s)}{\delta s} g_0(s) = \begin{bmatrix} 0 & -\cos s_2 & 0 \end{bmatrix} \begin{bmatrix} 0 \\ 0 \\ 1 \end{bmatrix} = 0$$

$$L_{g_0}L_{f_0}^2h(s) = \frac{\delta L_{f_0}^2h(s)}{\delta s}g_0(s) = \begin{bmatrix}0 & 0 & k\sin s_3\end{bmatrix}\begin{bmatrix}0\\0\\1\end{bmatrix} = k\sin s_3$$

$$\Rightarrow \textit{ Relative Degree, } \rho = 3 = n \tag{5}$$

$$L_{f_0}^3h(s) = \frac{\delta L_{f_0}^2h(s)}{\delta s}f_0(s) = \begin{bmatrix}0 & 0 & k\sin s_3\end{bmatrix}\begin{bmatrix}-\sin s_2\\k\cos s_3\sec s_2\\-k\cos s_3\tan s_2\end{bmatrix}$$

$$= -k^2\sin s_3\cos s_3\tan s_2$$

Now, by **Input-Output Feedback Linearization**, $r = T(s) = \begin{bmatrix}\eta\\\xi\end{bmatrix}$. Since, relative degree $\rho = n = 3$, η does not exist and $T(s) = \xi$.

$$r = T(s) = \xi = \begin{bmatrix}h(s)\\L_{f_0}h(s)\\L_{f_0}^2h(s)\end{bmatrix}$$

$$r = \begin{bmatrix}r_1\\r_2\\r_3\end{bmatrix} = \begin{bmatrix}s_1\\-\sin s_2\\-k\cos s_3\end{bmatrix}$$

$$\begin{aligned}\dot{r_1} &= r_2\\ \dot{r_2} &= r_3\\ \dot{r_3} &= \nu_1 = f(r) + g(r)i\end{aligned} \tag{6}$$

$$,where,\ \nu_1 = \gamma(s)(i - \alpha(s))$$

$$\gamma(s) = L_{g_0}L_{f_0}^2h(s) = k\sin s_3$$

$$\alpha(s) = \frac{-L_{f_0}^3h(s)}{L_{g_0}L_{f_0}^2h(s)} = \frac{k^2\sin s_3\cos s_3\tan s_2}{k\sin s_3} = k\cos s_3\tan s_2$$

$$\Rightarrow \nu_1 = -k^2\sin s_3\cos s_3\tan s_2 + k\sin s_3 i$$

$$\begin{aligned}\dot{r_1} &= r_2\\ \dot{r_2} &= r_3\\ \dot{r_3} &= \nu_1 = f(r) + g(r)i + d\end{aligned} \tag{7}$$

$$f(r) = k\sin\left[\cos^{-1}\left(\frac{-r_3}{k}\right)\right]r_3\tan\left[\sin^{-1}(-r_2)\right]$$

$$g(r) = k\sin\left[\cos^{-1}\left(\frac{-r_3}{k}\right)\right]$$

$$Disturbance,\ d = 2\sin t + 3$$

Here, the disturbance considered in the model of the needling system d is matched Lipschitz continuous, and it is also assumed to be bounded where $||d(t)|| \leq d_m$ with known upper bound $d_m > 0$ and $||\dot{d}(t)|| \leq \tau$. The desired equilibrium state is $r = [0\ 0\ 0]^T$ corresponding to $s = \left[0\ 0\ \frac{\pi}{2}\right]^T$.

C. Conventional Sliding Mode Control

The sliding surface has been considered as follows:

$$\begin{aligned} \zeta &= c_1 r_1 + c_2 r_2 + r_3 \\ \dot{\zeta} &= c_1 r_2 + c_2 r_3 + f(r) + g(r) i + d \\ i &= -g^{-1}(r)[c_1 r_2 + c_2 r_3 + f(r) + K sign(\zeta) + \eta\zeta] \\ \Rightarrow\ \dot{\zeta} &= -K sign(\zeta) - \eta\zeta + 2\sin t + 3 \end{aligned} \tag{8}$$

The parameters $c_1 = 10,\ c_2 = 5,\ K = 6,\ \eta = 4$ give a desired rate of convergence of states to zero [1]. It is observed that there is **significant chattering** both **with and without disturbance**. This is because of the discontinuity in control input. Thus, in the next subsections, we try to make the control input continuous.

D. Continuous Finite-time Feedback Control With and Without Disturbance

According to [6], there exists a continuous finite-time stabilization feedback control for a chain of integrator systems. According to **Proposition 8.1 [6] :**

Theorem 1 [6]. *Let $a_1, ...a_n > 0$ be such that the polynomial $\Gamma^n + a_n\Gamma^{n-1} + ... + a_2\Gamma + a_1$ is **Hurwitz**, and there exists $\epsilon \in (0,1)$ such that, for every $b \in (1-\epsilon, 1)$, the **origin** is a **globally finite-time stable equilibrium** for the undisturbed system* (6) *under the feedback control $i = g^{-1}(r)[u - f(r)]$ by assuming:*

$$u = -a_1|r_1|^{b_1} sign(r_1) - ... - a_n|r_n|^{b_n} sign(r_n) \tag{9}$$

,where, $b_1, ..., b_n$ satisfy

$$b_{w-1} = \frac{b_w b_{w+1}}{2b_{w+1} - b_w},\ w = 2, .., n \tag{10}$$

, with, $b_{n+1} = 1$ and $b_n = b$.

The **proof** is based on **Lyapunov Global Asymptotic stabilty** and a lot of theorems derived in [6] that relate it to **Finite-time stability**. To understand the need for ISMC, first the control law in (7) was applied with $i = g^{-1}(r)[u - f(r)]$ and control $u = u_{nom}$, the nominal control input defined below in (11) with state as $r = [r_1\ r_2\ r_3]^T$.

$$u_{nom} = -a_1|r_1|^{b_1} sign(r_1) - a_2|r_2|^{b_2} sign(r_2) - a_3|r_3|^{b_3} sign(r_3) \tag{11}$$

, where, controller gains were chosen as $a_1 = 15,\ a_2 = 23,\ a_3 = 9$, $b_1 = \frac{1}{4},\ b_2 = \frac{1}{3},\ b_3 = \frac{1}{2}$. It is observed that the nominal control with these control gains makes the states r converge to zero in desired finite-time when there is **no disturbance** d. But, when there is **disturbance** $d = 2\sin t + 3$ states **do not converge** to the equilibrium point in finite-time. Also, it is observed that the frequency of chattering is reduced significantly. So, we just need to take care of the disturbance rejection now. So we try to implement **Integral SMC (ISMC)** with a **discontinuous control input** to **reject the disturbance**.

E. ISMC With Discontinuous Control

In Integral SMC (ISMC), the control input has **2 parts**. First is the **continuous control** component known as nominal control input (u_{nom}). Second is the discontinuous control (u_{discon}). The **discontinuous control term** takes care of **disturbance rejection** while the **continuous control term** is reponsible for the **reduced chattering performance** of the system.

The controller design is as follows:

$$\begin{aligned} u &= u_{nom} + u_{discon} \\ u_{discon} &= -a_4 sign(\zeta) \\ Sliding\ variable,\ \zeta &= r_3 - r_{30} - \int_0^t u_{nom} dt,\ r_{30}\ is\ initial\ condition\ of\ r_3 \\ \Rightarrow\ \dot{\zeta} &= u + d - u_{nom} = 0 \\ \Rightarrow\ u_{nom} + u_{discon} + d - u_{nom} &= 0 \\ \Rightarrow\ u_{discon} &= -d \\ \Rightarrow\ [-a_4 sign(\zeta)]_{eq} &= -d \end{aligned} \tag{12}$$

Thus, the trajectory **starts from the sliding surface**. Also, the u_{discon} is negative of disturbance d and hence should reject the disturbance. $a_4 = 10$ is considered for the simulation. However, we still face the issue that the control input is discontinuous in nature which will cause chattering.

F. Proposed Controller: ISMC with STA / STC

1) Intro to STA and proof of Finite-time convergence: Higher Order SMC means that the equation for the higher order derivative of sliding variable must contain the discontinuity such that all lower derivatives converge to zero in finite-time. The **sliding manifold** in this type of control is **not just** $\zeta = 0$ but is:

$$\Phi = \{\zeta = 0, \frac{d^e \zeta}{dt^e} = 0,\ e = 1, .., m-1\} \tag{13}$$

, where, m is order of sliding-mode. Solving this problem of **higher-order sliding mode control** is a nontrivial task. Some popular algorithms used for this purpose are twisting algorithm, sub-optimal algorithm, control law with prescribed convergence law, terminal sliding mode controller and super twisting controller. Out of these, the most popular is **super twisting algorithm (STA)**.

The **assumptions** in **STA** are as follows [7]:

$$\begin{aligned} &Sliding\ variable,\ \dot{\zeta} = h_1(x) + g_1(x)u + d(t) \\ &u = -\lambda|\zeta|^{1/2} sign(\zeta) + \nu \\ &\dot{\nu} = \begin{cases} -u, & |u| > U_M \\ -\alpha sign(\zeta), & |u| \leq U_M \end{cases} \\ &|\dot{h_1}| + |\dot{g_1}|U_M + |\dot{d}(t)| \leq C \\ &0 < K_m \leq g_1(x) \leq K_M \\ &|h_1| < q|g_1|U_M,\ q \in (0,1) \\ &|\dot{d}(t)| \leq C_1 \\ &|d(t)| \leq C_2 \end{aligned} \tag{14}$$

The **STA** is also sometimes written as follows with the assumption that magnitude of the input u is always bounded with a known upper bound U_M. [5] [4] [1]:

$$\begin{aligned} &Sliding\ variable,\ \dot{\zeta} = h_1(x) + g_1(x)u + d(t) \\ &u = -\lambda|\zeta|^{1/2} sign(\zeta) + \nu \\ &\dot{\nu} = -\alpha sign(\zeta) \end{aligned} \tag{15}$$

We know that $d(t)$ satisfies the assumptions $|d(t)| \leq C_2$ and $|\dot{d}(t)| \leq C_1$, with, $C_1 = \tau$ and $C_2 = d_m$ as given in the paper [1]. The **conditions on controller gains** are given below:

$$\begin{aligned} &K_m\alpha > C \\ &\lambda > \sqrt{\frac{2}{K_m\alpha - C}} \times \frac{K_m\alpha + C}{K_m} \times \frac{1+q}{1-q} \end{aligned} \tag{16}$$

These conditions and assumptions help in the **proof of finite-time stability of the STA** which is based on **majorant curve analysis [5] [7]**. For the purpose of this paper, the simplest case of STA is considered where $h_1(x) = 0,\ g_1(x) = 1$.

Majorant Curve Analysis:

If we consider $x_1 = \zeta$, $x_2 = \dot{\zeta}$,

$$\begin{aligned} \dot{x_1} &= x_2 \\ \dot{x_2} &= \dot{h_1}(x) + \dot{g_1}(x)u + g_1(x)\dot{u} \\ &= [-C, C] - [K_m, K_M]\left(\frac{\lambda x_2}{2|x_1|^{1/2}} + \alpha sign(x_1)\right) \end{aligned} \tag{17}$$

Proof of Finite-time Stability:

When $|u| > U_M$,

$$\dot{u} = -\frac{\lambda}{2}\frac{\dot{\zeta}}{|\zeta|^{1/2}} - u$$

$$\begin{aligned} &Since\ |h_1| < q|g_1|U_M,\ contribution\ of\ h_1(x)\ in\ \dot{\zeta}\ is\ less \\ &\Rightarrow sign(\dot{\zeta}) = sign(u)\ \Rightarrow \dot{s}u\ =\ 0 \\ &\Rightarrow u\dot{u} = -\frac{\lambda}{2}\frac{\dot{\zeta}u}{|\zeta|^{1/2}} - u^2 \\ &\Rightarrow u\dot{u} < 0 \end{aligned} \tag{18}$$

Thus, u enters the bound $[-U_M, U_M]$ and never leaves.

When $|u| \leq U_M$,

$$\dot{\zeta} = \dot{h_1} + \dot{g_1}u - g_1\left(\frac{\lambda}{2}\frac{\dot{\zeta}}{|\zeta|^{1/2}} + \alpha sign(\zeta)\right)$$

$$\begin{aligned} &Let\ x_1 = \zeta,\ x_2 = \dot{\zeta}, \\ &\dot{x_1} = x_2 \\ &\dot{x_2} = [-C, C] - [K_m, K_M]\left(\frac{\lambda}{2}\frac{x_2}{|x_1|^{1/2}} + \alpha sign(x_1)\right) \end{aligned} \tag{19}$$

Quadrant 1 (Q-1)

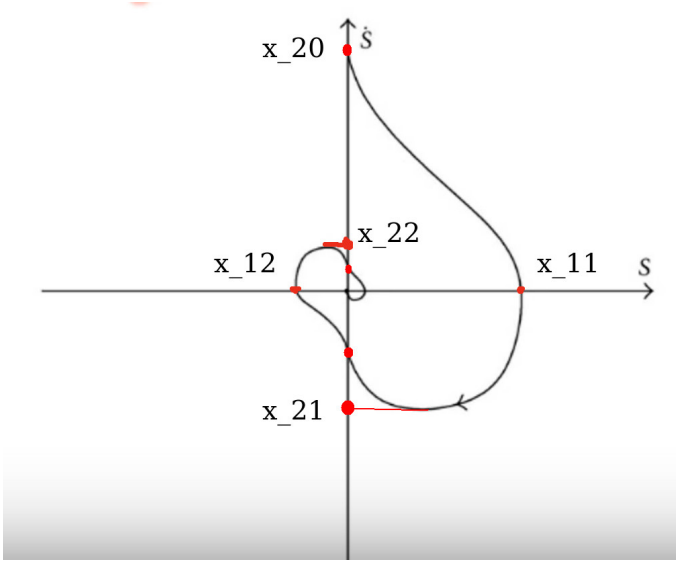

Fig. 3. Super Twisting Algorithm (STA) ζ v/s $\dot{\zeta}$ [7]

As can be seen in Fig. 3, initial point is $(0, x_{20})$. $x_1 > 0, x_2 > 0$. **Worst case** is when $\dot{x_2}$ is maximum.

$$\begin{aligned} \dot{x_2}|_{max} &= C - K_m\alpha < 0 \ \Rightarrow x_2 \ is \ decreasing \\ \frac{dx_2}{dx_1} &= \frac{C - K_m\alpha}{x_2} \\ \int_{x_{20}}^{0} x_2 dx_2 &= (C - K_m\alpha) \int_0^{x_{11}} dx_1 \\ |x_{20}| &= \sqrt{2(K_m\alpha - C)} \ |x_{11}|^{1/2} \\ \int_{x_{20}}^{0} dx_2 &= (C - K_m\alpha) \int_0^{t_1} dt \\ t_1 &= \frac{x_{20}}{K_m\alpha - C} \end{aligned} \tag{20}$$

Quadrant 4 (Q-4)

As can be seen in Fig. 3, initial point is $(0, x_{11})$. $x_1 > 0, x_2 < 0$. **Worst case** is when $\dot{x_2}$ is minimum.

$$\dot{x_2}|_{min} = -C + K_m \frac{\lambda}{2} \frac{|x_2|}{|x_1|^{1/2}} - K_m\alpha \tag{21}$$

From negative, $\dot{x_2}$ goes to zero and then becomes positive. Hence, it approaches x_2 axis. To check the lowest bound, we note that $\dot{x_2} = 0$ there and $|x_2| = |x_{21}|$. Thus,

$$\begin{aligned} |x_{21}| &= \frac{2(K_m\alpha + C)}{\lambda K_m} |x_{11}|^{1/2} \\ \dot{x_1} = x_2 &= \frac{-2(K_m\alpha + C)}{\lambda K_m} x_1^{1/2} \\ \int_{x_{11}}^{0} x_1^{-1/2} dx_1 &= \frac{-2(K_m\alpha + C)}{\lambda K_m} \int_0^{t_2} dt \\ t_2 &= \frac{\lambda K_m |x_{11}|^{1/2}}{4(K_m\alpha + C)} \\ &= \frac{\lambda K_m |x_{20}|}{4(K_m\alpha + C)\sqrt{2(K_m\alpha - C)}} \end{aligned} \tag{22}$$

Combining equations Eq. (20) and Eq. (22) from Quadrants 1 and 4 majorant curve analysis, we get:

$$\begin{aligned} \frac{|x_{21}|}{|x_{20}|} &= \sqrt{\frac{2}{K_m\alpha - C}} \ \frac{K_m\alpha + C}{\lambda K_m} \\ &< \ \frac{1-q}{1+q} \ = \ r \ < \ 1 \ from \ conditions \ and \ assumptions \\ \Rightarrow \frac{|x_{21}|}{|x_{20}|} &< 1 \end{aligned} \tag{23}$$

Similarly, it can be shown that $\frac{|x_{2(i+1)}|}{|x_{2i}|} \ = \ r < 1$ This means that x_2, i.e., $\dot{\zeta}$ **converges** to zero but in **infinite steps**.

Time taken between x_2 axis crossing is a multiple of $|x_{20}|$

$$\begin{aligned} T_1 &= t_1 + t_2 = p|x_{20}| \\ Similarly, \ T_{i+1} &= p|x_{2i}| \\ Total \ Time \ Of \ Convergence, \ T &= \Sigma_{i=1}^{\infty} T_i \ = \ p|x_{20}|\Sigma_{i=0}^{\infty} r^i \\ T &= \frac{p|x_{20}|}{1-r} > 0 \ and \ finite \end{aligned} \tag{24}$$

Thus, **although** it takes **infinite steps**, it takes **finite time** to **converge**. Thus, **finite-time stability of STA** is proved. **Q.E.D.**

2) Integrating ISMC with STA for given system: Here, we replace the discontinuous term in ISMC by STA control term.

$$\begin{aligned} u &= u_{nom} + u_{STC},\ \dot{\zeta} = u + d - u_{nom} \\ \dot{\zeta} &= u_{STC} + d,\ u_{STC} = -a_5|\zeta|^{1/2} sign(\zeta) + \Theta \\ \dot{\zeta} &= -a_5|\zeta|^{1/2} sign(\zeta) + \Theta + d,\ \dot{\Theta} = -a_6 sign(\zeta) \\ O &= \Theta + d,\ \dot{\zeta} = -a_5|\zeta|^{1/2} sign(\zeta) + O \\ \dot{O} &= -a_6 sign(\zeta) + \dot{d} \end{aligned} \tag{25}$$

For simulation, we choose $a_5 = 0.13,\ a_6 = 300$ controller gains, withwhich we can conclude finite-time convergence to $\zeta = O = 0$. By using the STC in integral sliding mode control, both the control signals are continuous in nature and we achieve a chattering-free response from the control input. It is observed that in spite of disturbances, we can get $\zeta = O = 0$ which gives us $\dot{\zeta} = 0$. Therefore,

$$\begin{aligned} \dot{\zeta} &= u + d - u_{nom} = 0 \\ \Rightarrow u + d &= u_{nom} \end{aligned} \tag{26}$$

Thus, we replace $u + d$ by u_{nom} which is free of disturbances in the chain of integrator form of state-space (7) having $i = g^{-1}(r)(u - f(r))$. Thus, we get almost chattering-free response and finite-time convergence to desired states. Thus,

$$u_{STC} = -d \tag{27}$$

Thus, u_{STC} is the negative of disturbance and hence, cancels it out. Now, when the system state trajectory is on the sliding surface, the dynamics of the system is governed by the nominal control input which is stable by its inherent design [6].

III. Simulation and Results

The simulation is performed in **MATLAB** using the **ode45** solver. The parameters/controller gains considered are $c_1 = 10,\ c_2 = 5,\ K = 6,\ \eta = 4, a_1 = 15,\ a_2 = 23,\ a_3 = 9, b_1 = \frac{1}{4},\ b_2 = \frac{1}{3},\ b_3 = \frac{1}{2}, a_4 = 10,\ a_5 = 0.13$ and $a_6 = 300$.

We simulate **4** seperate **control strategies**:

- **Conventional SMC**
- **Continuous SMC without disturbance**
- **Continuous SMC with disturbance**
- **Integral SMC (ISMC) with Discontinuous Control**
- **ISMC with Super Twisting Algorithm (STA)**

A. r_1 State representing distance from xz plane

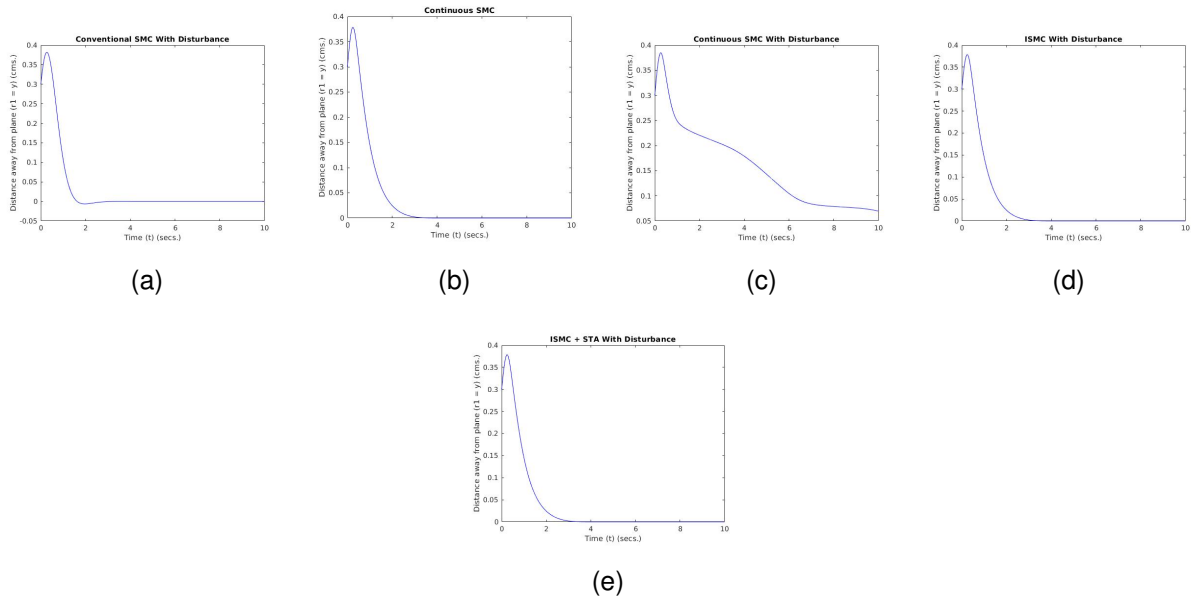

Fig. 4. Response of r_1 in (a) Conventional SMC, (b) Continuous SMC without disturbance, (c) Continuous SMC with disturbance, (e) ISMC with Discontinuous Control and (f) ISMC with STA

The Fig.4 shows that the r_1 state converges to zero in all the cases except for the case where we use Continuous Finite-Time Feedback Nominal Control in the presence of disturbance $d = 2\sin t + 3$. In Continuous Nominal Control case, in presence of disturbance, the state does not converge to zero. r_1 converging to zero means the distance from xz plane in y direction $s_1 = y$ converges to zero.

B. r_2, r_3 States representing rotations

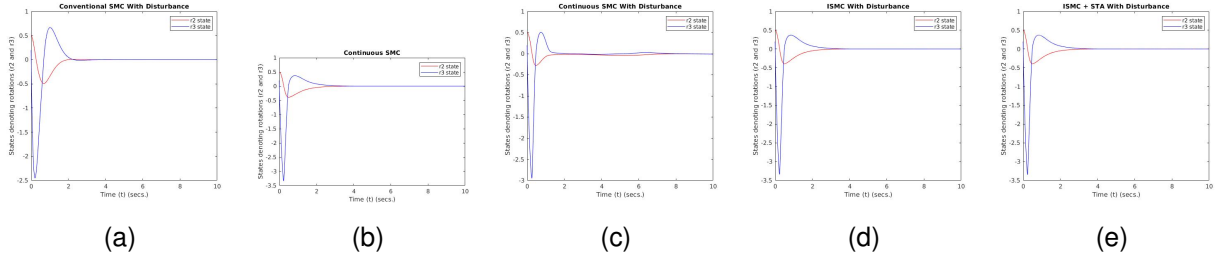

Fig. 5. Response of r_2 (red) and r_3 (blue) in (a) Conventional SMC, (b) Continuous SMC without disturbance, (c) Continuous SMC with disturbance, (e) ISMC with Discontinuous Control and (f) ISMC with STA

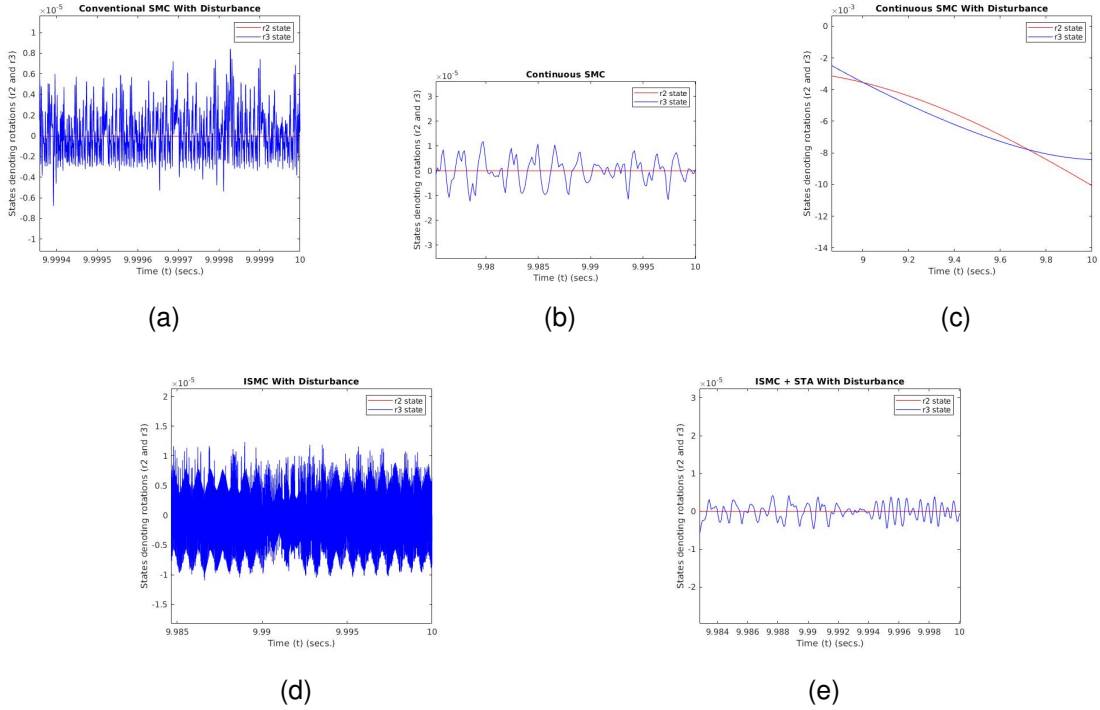

Fig. 6. Zoomed figures of Response of r_2 and r_3 in (a) Conventional SMC, (b) Continuous SMC without disturbance, (c) Continuous SMC with disturbance, (e) ISMC with Discontinuous Control and (f) ISMC with STA

The figures Fig.5 and Fig.6 show the plots of the states representing orientations $r_2$and r_3. r_2 and r_3 converging to zero means that the yaw converges to 0 and roll converges to $\frac{\pi}{2}$. We can clearly see in Fig. 6, there is **lot of chattering** in **Conventional SMC and in Integral SMC (ISMC)** with discontinuous control due to the discontinuity in control input. As expected, **Continuous control** has **significantly reduced chattering** and has finite-time convergence in absence of disturbance, but states **do not converge when disturbance is present**. **ISMC with STA reduces the chattering** significantly while also getting **finite-time convergence** even in presence of the disturbance.

We can observe Asymptotic Stability with Chattering for Conventional SMC, Finite-time stability without chattering

for Continuous Control in absence of disturbance and ISMC+STA, Finite-time stability with chattering for ISMC with discontinuous control and no convergence in Continuous Control in presence of disturbance although without any chattering.

C. Control Input

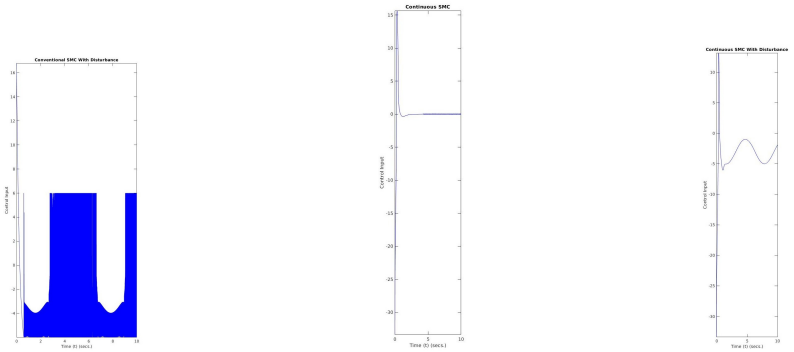

Fig. 7. Control Input in (a) Conventional SMC, (b) Continuous SMC without disturbance, (c) Continuous SMC with disturbance

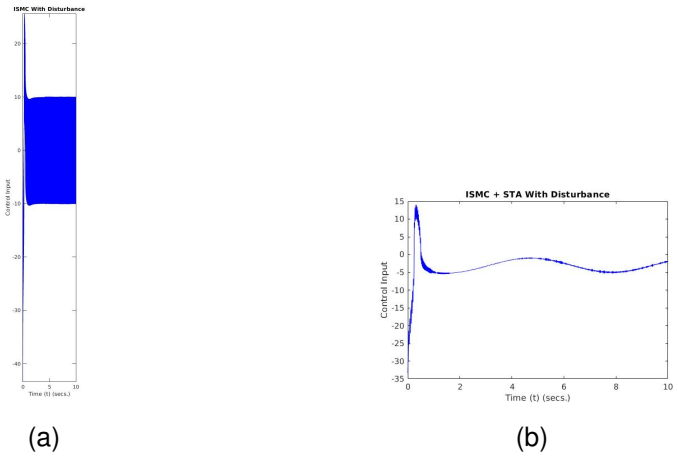

Fig. 8. Control Input in (a) ISMC with Discontinuous Control and (b) ISMC with STA

We can see the Control inputs in Fig. 7 and Fig. 8 which is as expected. We can see the chattering the control inputs for Conventional SMC and ISMC with Discontinuous Control. We can see that there is almost no chattering in Continuous SMC in absecnce of disturbance and ISMC with STA. We can see the sinuosoidal nature of control input in ISMC with STA control input since the STA part of the control input would be negative of the disturbance which is sinuosoidal.

D. Sliding Surface

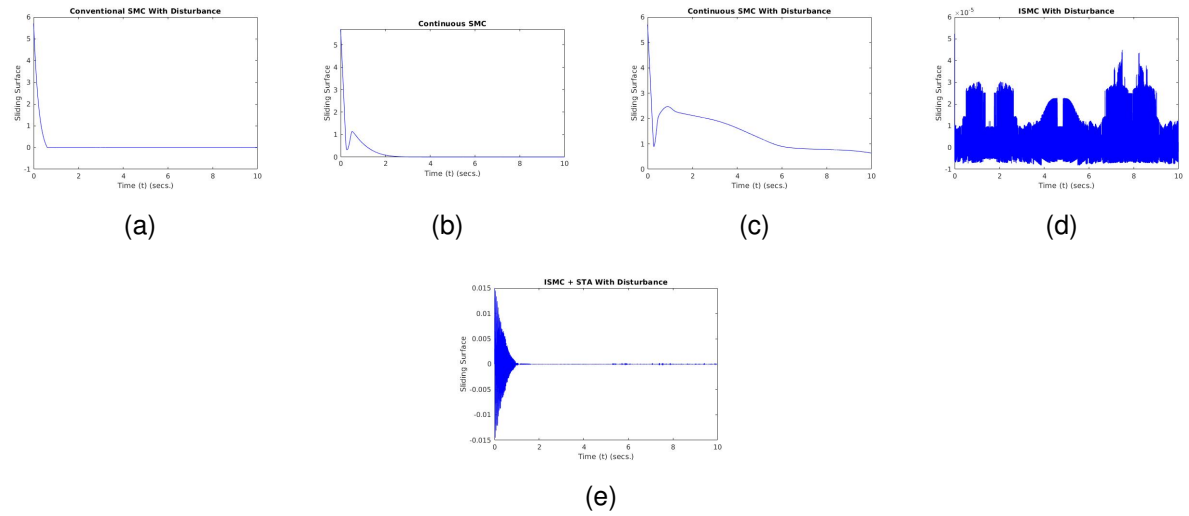

Fig. 9. Sliding Variable ζ in (a) Conventional SMC, (b) Continuous SMC without disturbance, (c) Continuous SMC with disturbance, (e) ISMC with Discontinuous Control and (f) ISMC with STA

E. Phase Portraits

Phase Portraits are shown in Fig. 10

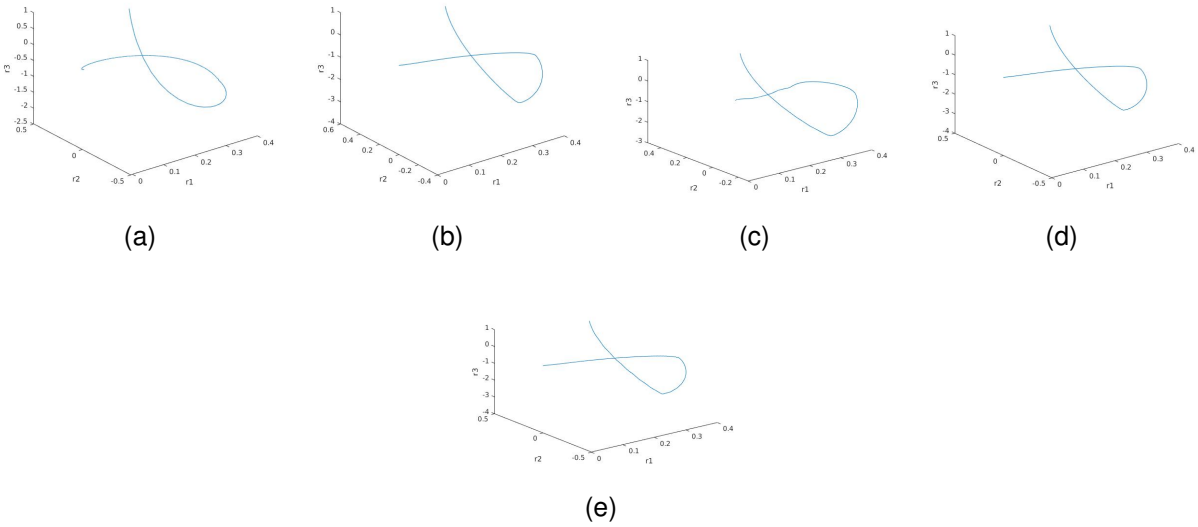

Fig. 10. Phase Portraits of r_1, r_2, r_3 in (a) Conventional SMC, (b) Continuous SMC without disturbance, (c) Continuous SMC with disturbance, (e) ISMC with Discontinuous Control and (f) ISMC with STA

F. Comparison

You can clearly see how much the chattering is reduced using ISMC with STA in Fig.11c.

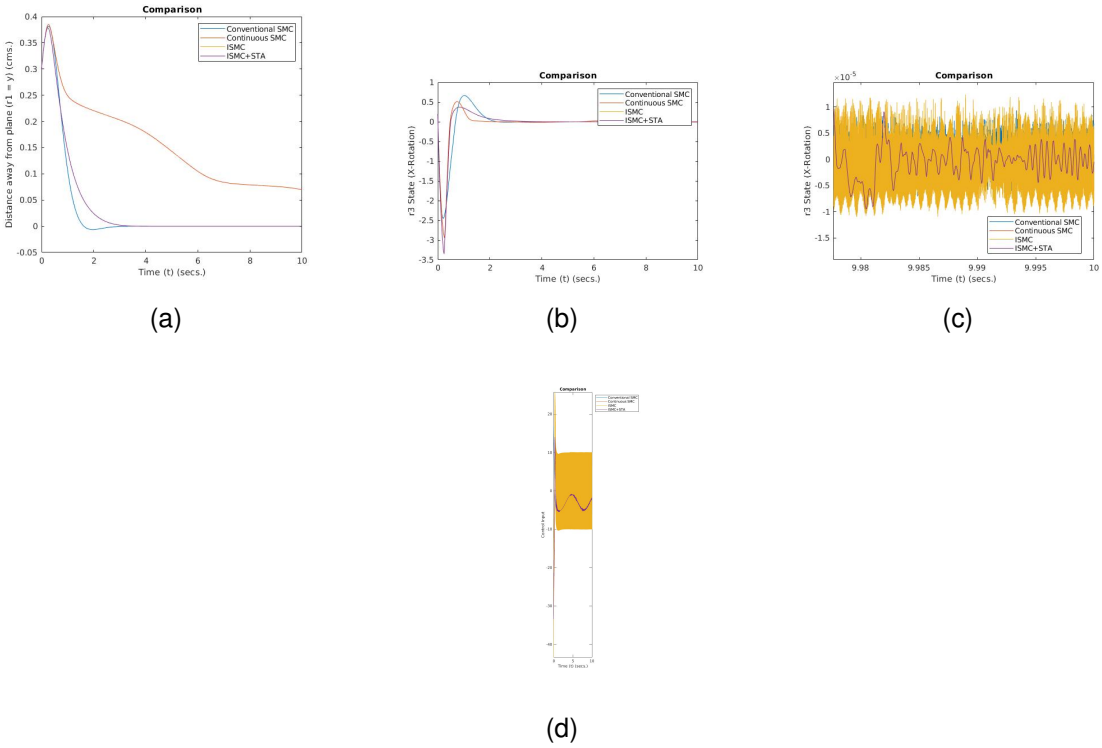

Fig. 11. Comparison of the various control strategies in (a) r_1, (b) r_3, (c) r_3 zoomed and (d) control u

IV. Conclusion

Hence, we can conclude that the proposed controller in the paper that uses Integral SMC (ISMC) with a continuous nominal control term and a Super Twisting control term gives finite-time convergence with almost no chattering.

REFERENCES

[1] S. Hans and F. O. M. Joseph, "Robust control of a bevel-tip needle for medical interventional procedures", IEEE/CAA Journal of Automatica Sinica, vol. 7, no. 1, pp. 244-256, January 2020, doi: 10.1109/JAS.2019.1911660.

[2] H.K. Khalil, Nonlinear Systems, 3rd edition, Prentice Hall, 2002.

[3] R. J. Webster, III, J. S. Kim, N. J. Cowan, G. S. Chirikjian, and A. M. Okamura, "Nonholonomic modeling of needle steering", Int. J. Robot. Res, vol. 25, no. 5/6, pp. 509–526, May/Jun. 2006.

[4] A. Moreno and M. Osorio, "Strict Lyapunov functions for the super-twisting algorithm," IEEE Trans. Automatic Control, vol. 57, no. 4, pp. 1035–1040, April 2012.

[5] A. Levant, "Robust exact differentiation via sliding mode technique", Automatica, vol. 34, pp. 379–384, 1998.

[6] S. P. Bhat and D. S. Bernstein, "Geometric homogeneity with applications to finite-time stability", Math. Control Signals Syst., vol. 17, no. 2, pp. 101–127, 2005

[7] Sohom Chakrabarty, "EEN613: Sliding Mode Control and Observation", IIT Roorkee, playlist link: https://www.youtube.com/playlist?list=PLJmxjP-2T4kvpU21YdGIrIXUYVjss1t0j

[8] D. C. Rucker, J. Das, H. B. Gilbert, P. J. Swaney, M. I. Miga, N. Sarkar, and R. J. Webster III, "Sliding mode control of steerable needles," IEEE Trans. Robot., vol. 29, no. 5, pp. 1289–1299, Oct. 2013.

[9] B. Fallahi, C. Rossa, R. S. Sloboda, N. Usmani, M. Tavakoli, "Sliding- based switching control for image-guided needle steering in soft tissue," IEEE Robot. Autom. Lett., vol. 1, no. 2, pp. 860–867, Jul. 2016.

[10] B. Fallahi, C. Rossa, R. S. Sloboda, N. Usmani, and M. Tavakoli, "Sliding based image-guided 3D needle steering in soft tissue," Control Eng. Pract., vol. 63, pp. 34–43, 2017.

[11] A. Majewicz, J. J. Siegel, A. A. Stanley, and A. M. Okamura, "Design and evaluation of duty-cycling steering algorithms for robotically-driven steerable needles," in Proc. IEEE Int. Conf. Robot. Autom. (ICRA), pp. 5883–5888, 2014.